International Journal of
Drug Discovery and Pharmacology（IJDDP）

Scilight

Article

Analyzing the Structure-Activity Relationship of Necrostain-1 and Its Analogues as RIPK1 Inhibitors on Necroptosis

Huilin Liu [1], Heng Wang [1], Haoyi Zheng [1], and Xiuping Chen [1,2,3,*]

[1] State Key Laboratory of Quality Research in Chinese Medicine, Institute of Chinese Medical Sciences, University of Macau, Macao, 519000, China
[2] Biological Imaging and Stem Cell Core, Faculty of Health Sciences, University of Macau, Taipa, Macao, 519000, China
[3] MoE Frontiers Science Center for Precision Oncology, University of Macau, Macao, 519000, China
* Correspondence: xpchen@um.edu.mo

Received: 6 October 2024; Revised: 5 November 2024; Accepted: 6 November 2024; Published: 20 June 2025

Abstract: Necroptosis is a type of programmed cell death mediated by the RIPK1-RIPK3-MLKL axis. Receptor-interacting serine/threonine-protein kinase 1 (RIPK1), the key upstream regulator of necroptosis, has been implicated in the pathogenesis of various diseases, and its inhibitors are being tested in clinical trials. Necrostatin-1 (Nec-1), the firstly identified RIPK1 inhibitor, effectively prevents necroptosis by specifically inhibiting the kinase activity of RIPK1. In our study, we compared the inhibitory efficiency of Nec-1 and its analogues on RIPK1 by using the TBZ-induced necroptosis model in HT29 cells and analyzing their structure-activity relationship (SAR). The results showed that Nec-1, Nec-1s, Nec-a1, Nec-a2, Nec-a3, Nec-a4, and Nec-a5 exhibited potent inhibition of TBZ-induced necroptosis and phosphorylation of RIPK1, RIPK3, MLKL. Molecular docking showed that there were two potential binding pockets between Nec-1 and its analogues with RIPK1. SAR analysis showed that the type and size of a substituent at the nitrogen atom in the 3-position of the imidazolidine ring markedly influenced the activity, indicating that a substituent at this position is essential for maintaining the biological function. This study helps to further elucidate how Nec-1 works and could lead to the development of more effective analogues.

Keywords: necroptosis; RIPK1; Necrostatin-1; molecular docking; SAR

1. Introduction

Cell death is indispensable for maintaining physiological homeostasis and can also manifest as an abnormal response to harmful stimuli [1]. Necroptosis is a regulated cell death (RCD) first proposed in 2005 [2,3]. The phosphorylation of mixed lineage kinase-like protein (MLKL) mediated by RIPK1 and Receptor-interacting serine/threonine-protein kinase 3 (RIPK3) has been established as an important signaling pathway for cell necroptosis (Figure 1A) [4–6]. The activation of cell surface death receptors, including Fas cell surface death receptors, TNF receptor 1 (TNFR1), Interferon-α/β receptor (IFNAR), and Toll-like receptors (TLRs), mediates necroptosis in response to inflammatory factors or infections [7]. Binding to death receptors activates RIPK1, which in turn activates RIPK3 by binding to RIPK3 through the shared RIP homologous interaction motif (RHIM) between the two molecules [8]. MLKL will be further activated by phosphorylation and form oligomers translocation to the cell plasma membrane, which finally causes cell membrane rupture, leakage of the intracellular components, and necroptosis [9–11]. The process of necroptosis is implicated in the pathological processes of inflammation, ischemia-reperfusion injury, and immune responses [12–14]. Therefore, targeting necroptosis is an ideal strategy for necroptosis-related diseases.

RIPK1 plays a pivotal role as both a regulatory and an upstream signaling molecule in the context of

necroptosis making it a prime target for modulating the progression [15–17]. While several RIPK1 inhibitors, such as DNL758, SIR1-365, R-522, and GSK2982772, are currently undergoing clinical trials, the clinical utility of many other RIPK1 inhibitors is limited by issues like cytotoxicity and unfavorable pharmacokinetic profiles [18, 19]. Thereby, this current situation emphasizes the continuous need to explore novel avenues with better specificity and higher inhibition efficiency in inhibiting RIPK1 kinase activity. Among these inhibitors, Nec-1 stands out due to its ability to occupy the allosteric pocket of RIPK1, thereby selectively modulating RIPK1 activity with significant kinase specificity [20]. This characteristic raises the possibility that Nec-1 analogues may also possess the capacity to inhibit RIPK1 effectively [21] (Figure 1A). However, SAR analysis of Nec-1 and its analogues remains unclear. In this study, we compared the inhibitory efficiency of Nec-1 and 8 its analogues (Figure 1B) on RIPK1 kinase activity by using the TBZ-induced necroptosis model in HT29 cell line and analyzing their SAR. This study helps to further elucidate how Nec-1 works and could lead to the development of more effective analogues.

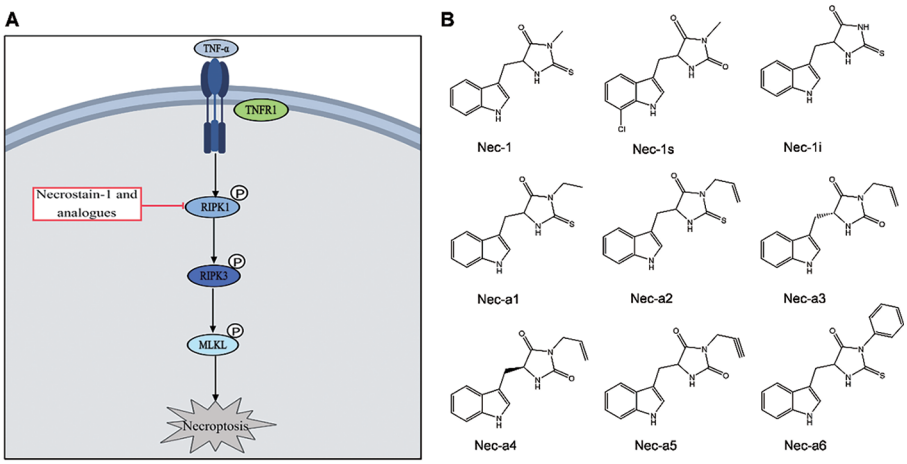

Figure 1. The necroptotic signaling pathway (**A**) and structure of Nec-1 and its analogues (**B**).

2. Materials and Methods

2.1. Chemicals and Reagents

Necrostatin-1 (Nec-1), Necrostatin-2 racemate (Nec-1s), and Necrostatin-1, inactive control (Nec-1i) were purchased from MedChemExpress (Shanghai, China). 3-ethyl-5-(1*H*-indol-3-ylmethyl)-2-thioxoimidazolidin-4-one (Nec-a1), 5-(1*H*-indol-3-ylmethyl)-3-(prop-2-en-1-yl)-2-thioxoimidazolidin-4-one (Nec-a2) were purchased from Vitas-M LABORATORY, (5R)-5-[(1*H*-indol-3-yl)methyl]-3-(prop-2-en-1-yl)imidazolidine-2,4-dione(Nec-a3), (5S) -5- [(1*H*-indol-3-yl)methyl] -3- (prop-2-en-1-yl)imidazolidine-2, 4-dione (Nec-a4), 5- [(1*H*-indol-3-yl) methyl] -3- (prop-2-yn-1-yl)imidazolidine-2, 4-dione (Nec-a5) were purchased from Chemspace, 5- (3-Indolylmethyl)-3-phenyl-2-thiohydantoin (Nec-a6) was purchased from TCI AMERICA. TNF-α was acquired from R&D Systems (Minneapolis, MI, USA). Z-VAD-FMK and BV6 were from Selleck (Shanghai, China). The antibodies were GAPDH **(**60004-1-ig, Proteintech), MLKL (14993S, CST), MLKL-pS358 (91689S, CST), RIPK1 (3493S, CST), RIPK1-s166 (44590S, CST), RIPK3(957020S, CST), RIPK3-s227 (ab209384, abcam).

2.2. Cell Culture

The human colorectal adenocarcinoma cell line HT29 purchased from the American Type Culture Collection (ATCC, Manassas, VA, USA) was cultured in McCoy's 5A Medium (Gibco, CA, USA) supplemented with 10% fetal bovine serum (Gibco, CA, USA), 1% penicillin, and 1% streptomycin in a controlled environment at 37 °C with 5% CO_2.

2.3. Cell Viability Assay

HT29 cells were cultured in a T75 flask with 10 mL of 5 A medium. The cell density was adjusted to 1.5 × 10^4 cells per well, and the cells were inoculated in a 96-well cell culture plate at a volume of 100 μL per well.

After overnight incubation, the cells were divided into two groups: the DMSO group and the TBZ group, both of which were treated with Nec-1 or its analogues (30 μM) for 1 h. Subsequently, the DMSO group was treated with DMSO and the TBZ group was exposed to a combination of TNF-α (20 ng/mL), BV6 (500 nM), and z-VAD-FMK (20 μM) to induce necroptosis. Both groups were then subjected to treatment for a total duration of 24 h. Following these treatments, the medium was replaced to include 1 mg/mL MTT and incubated at 37 °C for 2 h. Subsequently, 100 μL of DMSO was added to dissolve the purple formazan product. Absorbance was measured at 570 nm using a FlexStation 3 Benchtop Multi-Mode Microplate Reader (Molecular Devices, Sunnyvale, CA, USA).

2.4. Propidium Iodide (PI) Staining

The cells were treated in the same manner and grouped as described in the preceding cell viability assay. After a 24-h treatment, the cells were transferred to fresh medium containing PI at a concentration of 5 μg/mL and incubated in the dark at room temperature for 10 min. Subsequently, the cells were gently washed twice with PBS. Images were acquired using the Incucyte S3 live-cell analysis system.

2.5. Western Blotting

HT29 cells were cultured overnight in a 6-well plate at a density of 7×10^5 cells per well. Following treatment with drugs and TBZ for 4 h, the medium was discarded, and each well was gently washed with PBS. Subsequently, 50 μL of RIPA lysis buffer containing phenylmethylsulfonyl fluoride (PMSF) at a concentration of 1∶100 and a phosphatase inhibitor cocktail at a dilution of 1∶50 were added to each well to lyse the cells. After that, protein concentrations were meticulously assessed using BCA protein assay kits and denatured at 99 °C for 8 min. The samples were then separated by means of 10% SDS-PAGE, transferred onto polyvinylidene fluoride (PVDF) membranes, and blocked with 5% nonfat milk for 2 h. The target blot was incubated with primary antibody diluted to 1∶1000 at 4 °C overnight, followed by incubation with secondary antibody diluted to 1∶3000 at room temperature for an additional period of 2 h. A sensitive substrate along with a ChemiDoc™ imaging system was employed to detect the target band.

2.6. Molecular Docking

We downloaded a 3D structure of the human RIPK1 from the RCSB Protein Data Bank (PDB ID: 4ITH). The X-ray crystal structure has a resolution of 2.25 Å. We employed AutoDock Vina for molecular docking. Each docking stimulation required twenty-four individual runs (exhaustiveness). Following the virtual screening, the results gave us a ranked list of ligands based on their binding energy(kcal/mol). The results were analyzed using Pymol and Ligplot.

2.7. Statistical Analysis

Statistical analyses were performed using GraphPad Prism 10.0 software (GraphPad Software, Inc., La Jolla, CA, USA). The unpaired Student's *t*-test, a widely recognized parametric method for comparing means of independent samples, was used to evaluate differences between the two groups. For analyzing variations among multiple groups, we used one-way ANOVA, a robust statistical technique capable of addressing complex interactions and main effects. Statistical significance was set at $\alpha = 0.05$, with $p < 0.05$ indicating significant differences [22].

3. Results

3.1. The Protective Effect of Nec-1 and Its Analogues on TBZ-Induced Necroptosis

Compared with the control group, Nec-1 and its analogues alone show no significant effect on HT29 cells morphology (Figure 2A). However, notable changes in cell morphology were observed in TBZ group, characterized by cell swelling, plasma membrane rupture. Nec-1, Nec-1s, Nec-a1, Nec-a2, Nec-a3, Nec-a4, and Nec-a5 treated groups showed relatively normal cellular morphology, whereas Nec-1i and Nec-a6 had no protective effect. This phenomenon was further validated by PI staining (Figure 3A, B). TBZ resulted in a significant PI penetration as evidenced by the red fluorescence which was inhibited by Nec-1, Nec-1s, Nec-

a1, Nec-a2, Nec-a3, Nec-a4, and Nec-a5 co-treatment. The MTT assay showed that Nec-1 and its analogues alone exhibit no significant cytotoxicity (Figure 4A). Pre-treatment with Nec-1, Nec-1s, Nec-a1, Nec-a2, Nec-a3, Nec-a4, and Nec-a5 led to a substantial inhibition of TBZ-induced cell viability with percentages of 77.1%, 78.0%, 81.2%, 79.7%, 76.1%, 79.8%, and 80.5% respectively (Figure 4B). Together, these results suggest that Nec-1, Nec-1s, Nec-a1, Nec-a2, Nec-a3, Nec-a4, and Nec-a5 have a significant protective effect against TBZ-induced necroptosis.

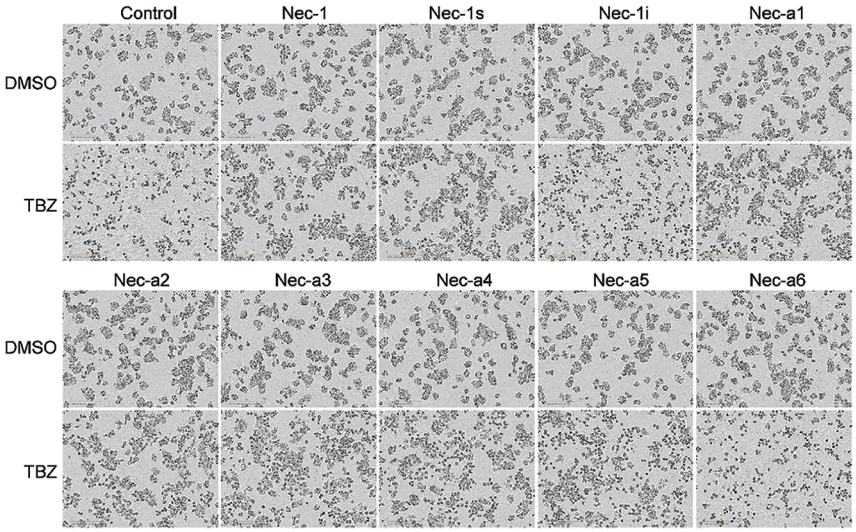

Figure 2. The inhibitory effect of Nec-1 and its analogues on TBZ-induced morphological changes. HT29 cells plated in 96-well plates were pretreated with Nec-1 and its analogues (30 μM) for 1h and then co-treated with TBZ for 24h. The morphology of the cells was imaged by an IncuCyte. TBZ: TNFα (20 ng/mL) + BV6 (500 nM) + z-VAD-FMK (20 μM), Scale bar = 200 μm.

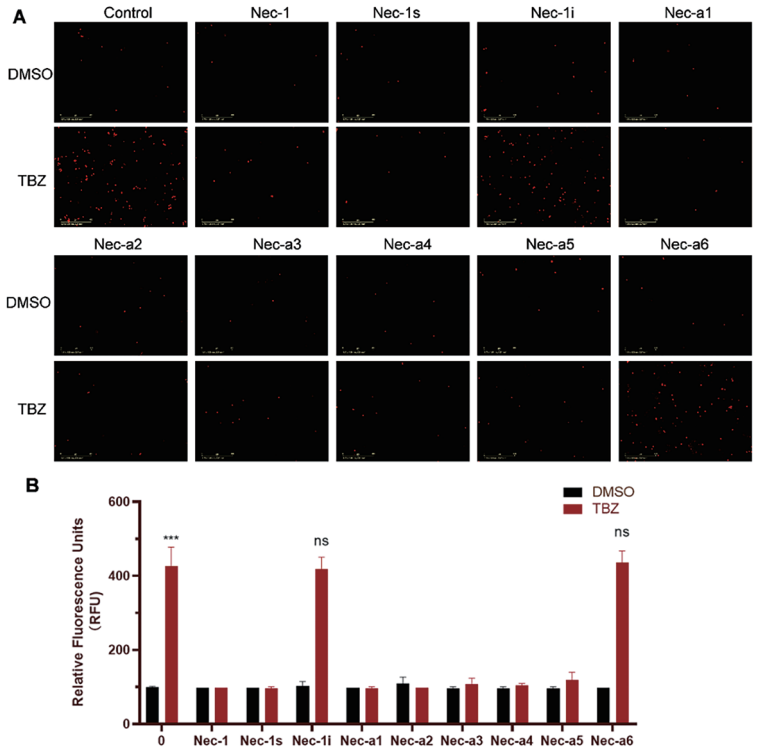

Figure 3. The inhibitory effect of Nec-1 and its analogues on TBZ-induced PI penetration. (**A**) HT29 cells were treated as described above and PI staining was performed. Scale bar = 400 μm. (**B**) Relative fluorescence units was quantified in each group. *** $p < 0.001$ vs. control group, *ns*, no significance vs. TBZ group.

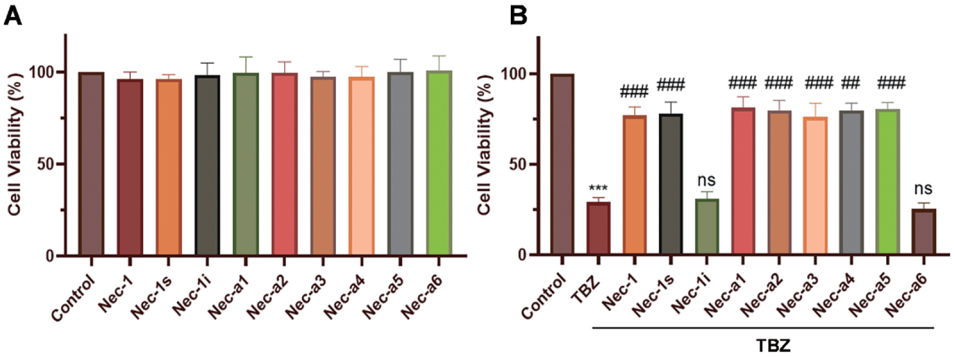

Figure 4. The inhibitory effect of Nec-1 and its analogues on TBZ-induced cell death in HT29 cells. (**A**) HT29 cells were treated with Nec-1 and its analogues (30 μM) for 24 h and cell viability was measured by MTT assay. (**B**) HT29 cells were pretreated with Nec-1 and its analogues for 1h and then co-treated with TBZ for 24h and the cell viability was determined by MTT assay. ***$p < 0.001$ vs. control group, $^{\#\#}p < 0.01$, $^{\#\#\#}p < 0.001$ vs. TBZ group, *ns*, no significance vs. TBZ group.

3.2. The Effect of Nec-1 and Its Analogues on Necroptotic Signal Pathway

As shown in Figure 5A,B, TBZ treatment markedly increased the protein expression of p-RIPK1, p-RIPK3, p-MLKL, which was significantly attenuated by Nec-1, Nec-1s, Nec-a1, Nec-a2, Nec-a3, Nec-a4, and Nec-a5 pretreatment. In contrast, neither Nec-1i nor Nec-a6 exhibited any inhibitory effect. These results indicated that Nec-1, Nec-1s, Nec-a1, Nec-a2, Nec-a3, Nec-a4, and Nec-a5 efficiently blocked TBZ triggered necroptosis mediated by the RIPK1-RIPK3-MLKL axis.

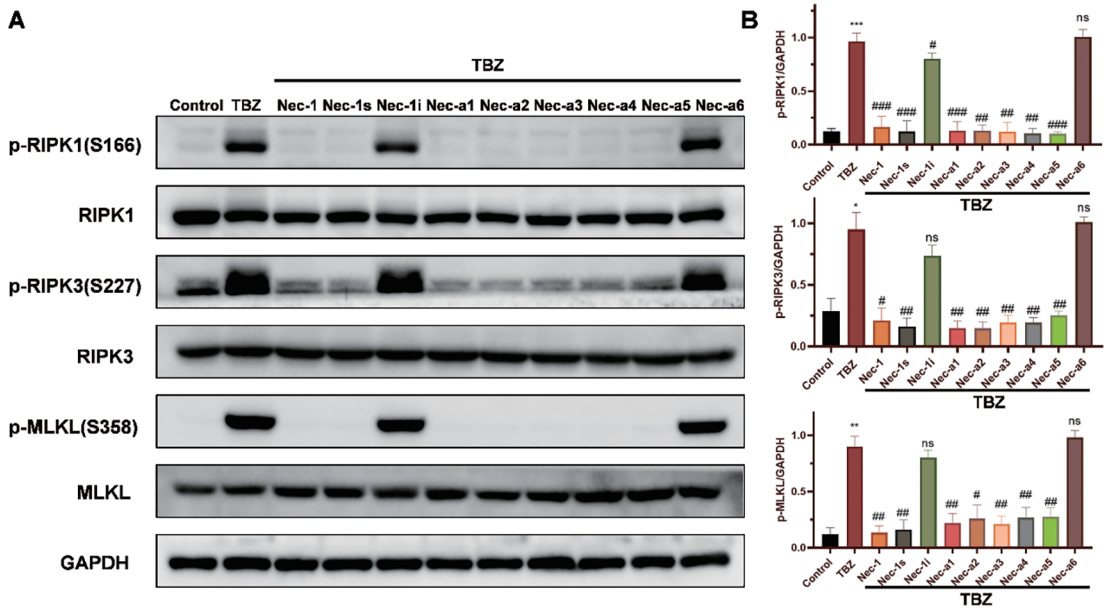

Figure 5. The effect of Nec-1 and its analogues on the protein expression of key proteins involved in necroptosis. (**A**) The cells were pre-treated with Nec-1 and its analogues (30 μM) for 1 h followed by TBZ co-treatment for 4 h. The protein expression was detected using Western blotting. (**B**) Quantitative analysis of the expression of p-RIPK1, p-RIPK3, p-MLKL. Data are shown as the means ± SD. *$p < 0.05$, ** $p < 0.01$, ***$p < 0.001$ vs. control group, $^{\#}p < 0.05$, $^{\#\#}p < 0.01$, $^{\#\#\#}p < 0.001$ vs. TBZ group, *ns*, no significance vs. TBZ group.

3.3. Molecular Docking of Nec-1 and Its Analogues with RIPK1

The molecular docking results of Nec-1 and its analogues with RIPK1 were shown in Figure 6A. Nec-1, Nec-1s, Nec-a1, and Nec-a2 had the same binding amino acid Glu 142 in a similar domain. In contrast, Nec-a3, Nec-a4, and Nec-a5 had different pocket binding with RIPK1, implying new potential target domain.

However, the binding of Nec-1i and Nec-a6 was not significant. The docking scores showed that Nec-a3 and Nec-a5 had the highest score while Nec-a6 and Nec-1i had the lowest scores (Figure 6B).

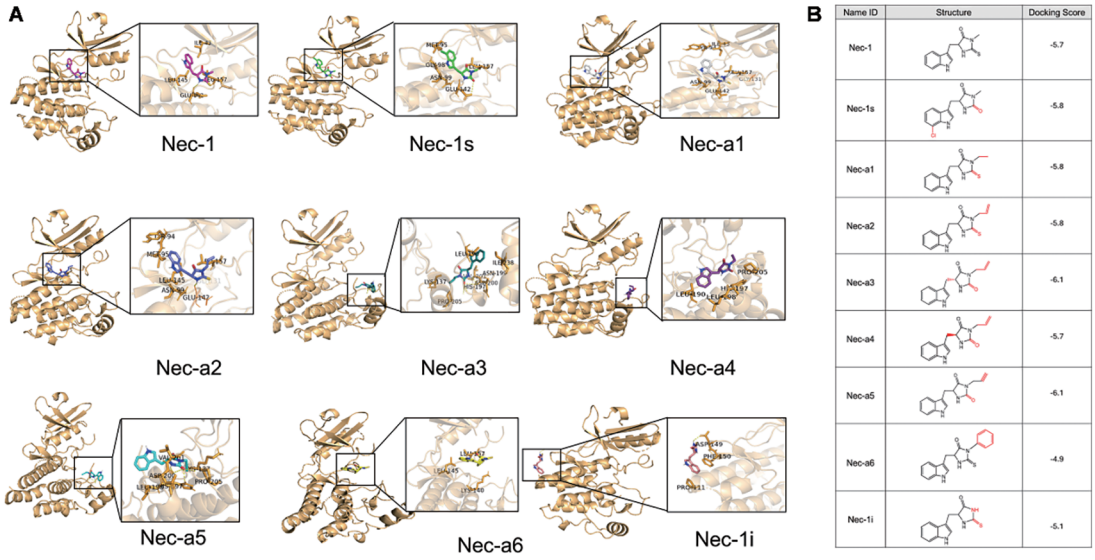

Figure 6. The molecular docking of Nec-1 and its analogues with RIPK1. (**A**) Molecular docking of Nec-1 and its analogues with RIPK1. Nec-1, Nec-1s, Nec-a1, and Nec-a2 showed a common binding mode and Nec-a3, Nec-a4, and Nec-a6 shared another new binding domain. (**B**) The binding score of Nec-1 and its analogues with RIPK1.

4. Discussion

RIPK1, a pivotal regulator of necroptosis, has emerged as a promising target in the realm of drug development. Currently, there exist three categories of RIPK1 inhibitors based on distinct binding sites. Among them, type I and type II inhibitors act by competitive binding to ATP sites of active and inactive RIPK1 conformations, respectively. Conversely, type III inhibitors modulate the activity of RIPK1 by occupying its allosteric pocket [23,24]. GSK′772, selected from GlaxoSmithKline libraries and DNA Encoded Compound Library, stands as the first RIPK1 inhibitor that has entered clinical trials with remarkable efficacy and tolerability in treating rheumatoid arthritis and active ulcerative colitis. Furthermore, potential drug candidates like SIR1-365, DNL788, and R-552 were in clinical trials thereby enhance the diversity for RIPK1 inhibitors [25,26].

Nec-1, a well-known small molecule, holds a prominent position as a representative RIPK1 inhibitor [27,28]. However, the poor pharmacokinetic properties of the Nec-1 series of compounds limited their subsequent development [29]. SAR analysis provides important insights into the molecular design of necrotic apoptosis inhibitors. In this study, the inhibitory effect of Nec-1 and its analogues on necroptosis was tested in a TBZ-triggered necroptosis model and the binding of them with RIPK1 was analyzed using molecular docking.

TBZ-triggered necroptosis model in HT29 cells has been well established. TBZ caused typical features of necroptosis, such as cell swelling, cell rupture, and leakage of contents [30,31]. Nec-1, Nec-1s, Nec-a1, Nec-a2, Nec-a3, Nec-a4, and Nec-a5 could significantly reverse the morphological changes induced by TBZ. PI, a fluorescent intercalating agent, can be used to stain nucleic acids of dead cells with incomplete membranes [32]. TBZ significantly induced PI penetration which was significantly inhibited by Nec-1, Nec-1s, Nec-a1, Nec-a2, Nec-a3, Nec-a4, and Nec-a5. Furthermore, similar inhibitory effect was observed in the MTT assay. In addition, Nec-1, Nec-1s, Nec-a1, Nec-a2, Nec-a3, Nec-a4, and Nec-a5 significantly decreased the phosphorylation of RIPK1, RIPK3, and MLKL triggered by TBZ. However, both Nec-1i and Nec-a6 showed no effect on TBZ-triggered cell death, RIPK1/3, MLKL phosphorylation. These results demonstrated that Nec-1, Nec-1s, Nec-a1, Nec-a2, Nec-a3, Nec-a4, and Nec-a5 were potent RIPK1 inhibitors while Nec-1i and Nec-a6 have no effect on RIPK1.

Molecular docking and SAR studies were conducted on Nec-1 and its analogues. Molecular docking

predicted that Nec-1, Nec-1s, Nec-a1, Nec-a2, Nec-a3, Nec-a4, and Nec-a5 had a robust binding effect with RIPK1, confirming the experimental results. However, the lowest docking scores of Nec-1i and Nec-a6 suggested their weak binding ability to RIPK1. Moreover, the docking pocket of Nec-a3, Nec-a4, and Nec-a5 with RIPK1 were different from those of Nec-1 and Nec-1s, suggesting that the inhibitory mechanisms may be different among Nec-1 and its analogues. The SAR showed that the substitution of thiadiazolidinone with the bioisosteric imidazolidinedione does not significantly alter biological activity suggesting that this structural modification has minimal influence on the compound's pharmacodynamics. However, the absence of a substituent at the nitrogen atom in the 3-position of the imidazolidine ring markedly decreases activity, indicating that a substituent at this position is essential for maintaining or enhancing the biological functions. Substituting the methyl group with alkyl (ethyl) or unsaturated hydrocarbon groups (alkenes or alkynes) at the same position preserved similar high biological activity, implying that within a specific chemical range, both the type and size of these substituents have little effect. In contrast, replacing the methyl group with a phenyl group leads to a complete loss of biological activity, thereby highlighting the adverse impact of aromatic substituents on the pharmacodynamic properties of this compound.

The above discussion is based on the results obtained from the human HT29 cell line. However, the existence of biological differences between animal models and human cells poses novel challenges for Nec-1 and its analogues in terms of development and SAR analysis. Moreover, the efficacy and safety profiles observed in animal models may also impact their translational potential for clinical applications. Therefore, future research should focus on thoroughly exploring these discrepancies to ensure successful advancement of Nec-1 and its analogues.

5. Conclusions

In conclusion, this study explored the effect and the SAR of Nec-1 and its analogues by evaluating their ability to inhibit necroptosis. The imidazolidine ring activity is significantly reduced by the absence of substituents or large substituents at nitrogen site 3. The results of this study provide novel insight for the design of new generation of RIPK1 inhibitors.

Author Contributions: H. L.: experiments, conceptualization, methodology, data curation, writing—original draft preparation. H.W.: investigation, validation. H.Z.: software. X.C.: conceptualization, supervision, writing—reviewing and editing. All authors have read and agreed to the published version of the manuscript.

Funding: This work was supported by the Science and Technology Development Fund, Macau SAR (0081/2021/A2), the Research Fund of University of Macau (MYRG-GRG2023-00072-ICMS-UMDF).

Institutional Review Board Statement: Not applicable.

Informed Consent Statement: Not applicable.

Data Availability Statement: Not applicable.

Acknowledgments: The authors thank Xiuping Chen at the ICMS, University of Macau, for his help and guidance.

Conflicts of Interest: The authors declare no potential conflict of interest.

References

1. Bertheloot, D.; Latz, E.; Franklin B.S. Necroptosis, pyroptosis and apoptosis: An intricate game of cell death. *Cell. Mol. Immunol.* **2021**, *18*, 1106–1121. https://doi.org/10.1038/s41423-020-00630-3.
2. Degterev, A.; Huang, Z.; Boyce, M.; et al. Chemical inhibitor of nonapoptotic cell death with therapeutic potential for ischemic brain injury. *Nat. Chem. Biol.* **2005**, *1*, 112–119. https://doi.org/10.1038/nchembio711.
3. Peng, F.; Liao, M.; Qin, R.; et al. Regulated cell death (RCD) in cancer: Key pathways and targeted therapies. *Signal Transduct. Target. Ther.* **2022**, *7*, 286. https://doi.org/10.1038/s41392-022-01110-y.
4. Zhang, D.W.; Shao, J.; Lin, J.; et al. RIP3, an energy metabolism regulator that switches TNF-induced cell death from apoptosis to necrosis. *Science* **2009**, *325*, 332–336. https://doi.org/10.1126/science.1172308.
5. Cho, Y.S.; Challa, S.; Moquin, D.; et al. Phosphorylation-driven assembly of the RIP1-RIP3 complex regulates programmed necrosis and virus-induced inflammation. *Cell* **2009**, *137*, 1112 – 1123. https://doi. org/10.1016/j. cell. 2009.05.037.
6. He, X.Y.; Wang, F.; Suo, X.G.; et al. Compound-42 alleviates acute kidney injury by targeting RIPK3-mediated necroptosis. *Br. J. Pharmacol*. **2023**, *180*, 2641–2660. https://doi.org/10.1111/bph.16152.
7. Vanlangenakker, N.; Vanden Berghe, T.; Vandenabeele, P. Many stimuli pull the necrotic trigger, an overview. *Cell Death Differ.* **2012**, *19*, 75–86. https://doi.org/10.1038/cdd.2011.164.

8. Vandenabeele, P.; Galluzzi, L.; Vanden Berghe, T.; et al. Molecular mechanisms of necroptosis: An ordered cellular explosion. *Nat. Rev. Mol. Cell Biol*. **2010**, *11*, 700–714. https://doi.org/10.1038/nrm2970.
9. Sun, L.; Wang, H.; Wang, Z.; et al. Mixed lineage kinase domain-like protein mediates necrosis signaling downstream of RIP3 kinase. *Cell* **2012**, *148*, 213–227. https://doi.org/10.1016/j.cell.2011.11.031.
10. Linkermann, A.; Green, D. R. Necroptosis. *N. Engl. J. Med.* **2014**, *370*, 455 – 465. https://doi. org/10.1056/NEJMra1310050.
11. Chen, X.; Li, W.; Ren, J.; et al. Translocation of mixed lineage kinase domain-like protein to plasma membrane leads to necrotic cell death. *Cell Res*. **2014**, *24*, 105–121. https://doi.org/10.1038/cr.2013.171.
12. Yuan, J.; Amin, P.; Ofengeim, D. Necroptosis and RIPK1-mediated neuroinflammation in CNS diseases. *Nat. Rev. . Neurosci.* **2019**, *20*, 19–33. https://doi.org/10.1038/s41583-018-0093-1.
13. Shan, B.; Pan, H.; Najafov, A.; et al. Necroptosis in development and diseases. *Genes Dev.* **2018**, *32*, 327–340. https://doi.org/10.1101/gad.312561.118.
14. Dong, L.; Liang, F.; Lou, Z.; et al. Necrostatin-1 Alleviates Lung Ischemia-Reperfusion Injury via Inhibiting Necroptosis and Apoptosis of Lung Epithelial Cells. *Cells* **2022**, *11*, 3139. https://doi.org/10.3390/cells11193139.
15. Mifflin, L.; Ofengeim, D.; Yuan, J. Receptor-interacting protein kinase 1 (RIPK*1*) as a therapeutic target. *Nat. Rev. Drug Discov.* **2020**, *19*, 553–571. https://doi.org/10.1038/s41573-020-0071-y.
16. Silke, J.; Rickard, J.A.; Gerlic, M. Erratum: The diverse role of RIP kinases in necroptosis and inflammation. *Nat. Immunol.* **2015**, *16*, 889. https://doi.org/10.1038/ni0815-889b.
17. Ju, E.; Park, K.A.; Shen, H.M.; et al. The resurrection of RIP kinase 1 as an early cell death checkpoint regulator-a potential target for therapy in the necroptosis era. *Exp. Mol. Med.* **2022**, *54*, 1401 – 1411. https://doi. org/10.1038/s12276-022-00847-4.
18. Zhang, L.; Li, Y.; Tian, C.; et al. From Hit to Lead: Structure-Based Optimization of Novel Selective Inhibitors of Receptor-Interacting Protein Kinase 1 (RIPK1) for the Treatment of Inflammatory Diseases. *J. Med. Chem.* **2024**, *67*, 754–773. https://doi.org/10.1021/acs.jmedchem.3c02102.
19. Tompson, D.J.; Davies, C.; Scott, N.E.; et al. Comparison of the Pharmacokinetics of RIPK1 Inhibitor GSK2982772 in Healthy Western and Japanese Subjects. *Eur. J. Drug Metab. Pharmacokinet*. **2021**, *46*, 71–83. https://doi.org/10.1007/s13318-020-00652-2.
20. Bai, Y.; Qiao, Y.; Li, M.; et al. RIPK1 inhibitors: A key to unlocking the potential of necroptosis in drug development. *Eur. J. Med. Chem*. **2024**, *265*, 116123. https://doi.org/10.1016/j.ejmech.2024.116123.
21. Chen, J.; Kos, R.; Garssen, J.; et al. Molecular Insights into the Mechanism of Necroptosis: The Necrosome As a Potential Therapeutic Target. *Cells* **2019**, *8*, 1486. https://doi.org/10.3390/cells8121486.
22. Vasamsetti, S.B.; Karnewar, S.; Kanugula, A.K.; et al. Metformin inhibits monocyte-to-macrophage differentiation via AMPK-mediated inhibition of STAT3 activation: Potential role in atherosclerosis. *Diabetes* **2015**, *64*, 2028–2041. https://doi.org/10.2337/db14-1225.
23. Weisel, K.; Scott, N. E.; Tompson, D. J.; et al. Randomized clinical study of safety, pharmacokinetics, and pharmacodynamics of RIPK1 inhibitor GSK2982772 in healthy volunteers. *Pharmacol. Res. Perspect.* **2017**, *5*. https://doi.org/10.1002/prp2.365.
24. Martens, S.; Hofmans, S.; Declercq, W.; et al. Inhibitors Targeting RIPK1/RIPK3: Old and New Drugs. *Trends Pharmacol. Sci.* **2020**, *41*, 209–224. https://doi.org/10.1016/j.tips.2020.01.002.
25. Xu, L.; Zhang, W.; Zhuang, C. Receptor-interacting protein kinase 1 (RIPK1inhibitor): A review of the patent literature (2018-present). *Expert Opin. Ther. Pat.* **2023**, *33*, 101–124. https://doi.org/10.1080/13543776.2023.2195548.
26. Rojas-Rivera, D.; Delvaeye, T.; Roelandt, R.; et al. When PERK inhibitors turn out to be new potent RIPK1 inhibitors: Critical issues on the specificity and use of GSK2606414 and GSK2656157. *Cell Death Differ.* **2017**, *24*, 1100–1110. https://doi.org/10.1038/cdd.2017.58.
27. Son, J.Y.; Ju, J.S.; Kim, Y.M.; et al. TNF-α-Mediated RIPK1 Pathway Participates in the Development of Trigeminal Neuropathic Pain in Rats. *Int. J. Mol. Sci*. **2022**, *23*, 506. https://doi.org/10.3390/ijms23010506.
28. Meng, H.; Wu, G.; Zhao, X.; et al. Discovery of a cooperative mode of inhibiting RIPK1 kinase. *Cell Discov.* **2021**, *7*, 41. https://doi.org/10.1038/s41421-021-00278-x.
29. Li, Z.; Hao, Y.; Yang, C.; et al. Design, synthesis, and evaluation of potent RIPK1 inhibitors with in vivo anti-inflammatory activity. *Eur. J. Med. Chem*. **2022**, *228*, 114036. https://doi.org/10.1016/j.ejmech.2021.114036.
30. Moriwaki, K.; Bertin, J.; Gough, P.J.; et al. Differential roles of RIPK1 and RIPK3 in TNF-induced necroptosis and chemotherapeutic agent-induced cell death. *Cell Death Dis*. **2015**, *6*, e1636. https://doi.org/10.1038/cddis.2015.16.
31. Gonçalves, J.; Amaral, J.D.; Capela, R.; et al. Necroptosis induced by ruthenium (II) complexes as mitochondrial disruptors. *Cell Death Discov.* **2024**, *10*, 261. https://doi.org/10.1038/s41420-024-02033-z.
32. Lecoeur, H. Nuclear apoptosis detection by flow cytometry: Influence of endogenous endonucleases. *Exp. Cell Res.* **2002**, *277*, 1–14. https://doi.org/10.1006/excr.2002.5537.